ACS APPLIED MATERIALS & INTERFACES

Research Article

www.acsami.org

Nanoscale Soldering of Axially Positioned Single-Walled Carbon Nanotubes: A Molecular Dynamics Simulation Study

Jianlei Cui,[†,‡] Lijun Yang,*[,†,‡] Liang Zhou,[‡] and Yang Wang*[,‡]

[†]Key Laboratory of Micro-systems and Micro-structures Manufacturing, Ministry of Education, Harbin Institute of Technology, Harbin 150001, China

[‡]School of Mechatronics Engineering, Harbin Institute of Technology, Harbin 150001, China

Supporting Information

ABSTRACT: The miniaturization of electronics devices into the nanometer scale is indispensable for next-generation semiconductor technology. Carbon nanotubes (CNTs) are considered to be the promising candidates for future interconnection wires. To study the carbon nanotubes interconnection during nanosoldering, the melting process of nanosolder and nanosoldering process between single-walled carbon nanotubes are simulated with molecular dynamics method. As the simulation results, the melting point of 2 nm silver solder is about 605 K because of high surface energy, which is below the melting temperature of Ag bulk material. In the nanosoldering process simulations, Ag atoms may be dragged into the nanotubes to form different connection configuration, which has no apparent relationship with chirality of SWNTs. The length of core filling nanowires structure has the relationship with the diameter, and it does not become longer with the increasing diameter of SWNT. Subsequently, the dominant mechanism of was analyzed. In addition, as the heating temperature and time, respectively, increases, more Ag atoms can enter the SWNTs with longer length of Ag nanowires. And because of the strong metal bonds, less Ag atoms can remain with the tight atomic structures in the gap between SWNT and SWNT. The preferred interconnection configurations can be achieved between SWNT and SWNT in this paper.

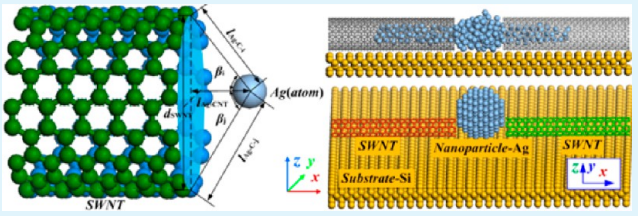

KEYWORDS: *carbon nanotube, interconnection, nanoscale soldering, molecular dynamics, silver nanosolder, core filling nanowires*

1. INTRODUCTION

According to the latest International Technology Roadmap for Semiconductors (ITRS),[1] with the development of the copper interconnects with smaller feature size, electro-migration become obvious because of the increasing current density, which could cause the damage and failure of electronic devices.[2,3] The miniaturization of electronics devices into the nanometer scale is indispensable for next generation semiconductor technology. Carbon nanotubes (CNTs) are considered to be the promising candidates for future interconnect wires with excellent physical and chemical properties ranging from ultrahigh mechanical strength, to electronic properties, to thermal conductivity, to optical properties, etc.[4−10] To obtain the effective mechanical and electrical connection, CNTs interconnect technology is essential for structure manufacturing and integration of nanofunctional devices. However, properly connected single-walled carbon nanotubes (SWNTs) could be the building blocks of various electronic devices, and the proper connection configurations of CNTs are critical for electrical and thermal transportation properties.[11−14] For the good interconnection configurations, some effective methods have been adopted by some researchers through C−C bonds connection, such as electron beam and ion beam nanowelding process.[15−18] But the CNTs are irradiated by high energy beam, the structures have large damages to induce high contact resistance and weak mechanical strength, which limits the practical applications. To overcome the adverse effects, it is necessary to take effective measurements to modify the interconnection configuration. Nanosoldering process has been founded as a more effective method with favorable electrical properties.

For achieving better interconnect quality, it is necessary to analyze the contact configuration modification between CNTs during nanowelding process. However, the determination of structures of CNTs interconnection is difficult to do experimentally. In contrast, molecular dynamics (MD) simulation provides a powerful method to investigate the structural and dynamical properties of interconnection points between CNTs in a realistic manner.[19−23] For example, Krasheninnikov performed ion beam welding process study by MD simulation.[17] Terrones used tight-binding MD simulations to study the coalescence of crossed CNTs and investigate the responsible mechanisms for the formation of the junction.[24] Additionally, Jang studied the electron beam nanowelding process of crossed CNTs revealed by MD simulation.[25] MD simulation is well suited to study irradiation process, as the time scales of the collisions and energy dissipation are on the order of picoseconds. Unfortunately,

Received: November 14, 2013
Accepted: January 6, 2014
Published: January 6, 2014

investigation of dynamic evolution of interconnection configuration is still lacking during nanosoldering. Consequently, nanoscale soldering of axially positioned SWNTs is reported in this Research Article. The main goal of our researches is to reveal nanoscale soldering process and the evolution interconnection configuration. Also, the dominant mechanism and detailed structural features were analyzed from different influence factors by a series of MD simulation results.

2. COMPUTATIONAL METHODOLOGY

To reveal the nanoscale soldering process of SWNTs in axial direction, the sketch map is presented in Figure 1. For MD simulation of

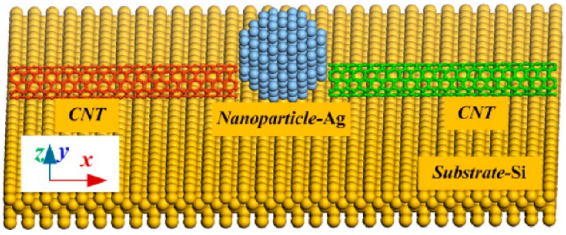

Figure 1. Sketch map of nanoscale soldering process of axially positioned carbon nanotubes.

evolution of connection configuration, various single-walled carbon nanotubes (SWNTs) with different spiral vector parameters and the same C−C atomic bond length of 1.42 Å are placed on the Si substrate of 3D cubic structure with lattice parameter of 5.4307 Å. Because the electrical and thermal properties of nanosolder are very important to interconnection configuration and performances, silver material becomes the focus of attention with the best electrical and thermal properties among many metal materials. Consequently, taking into account the diameter size of the SWNT, for avoiding more solders to have a marked impact on the adjacent interconnect wires, one Ag nanoparticle shown in Figure 2, was chosen as nanosolder during

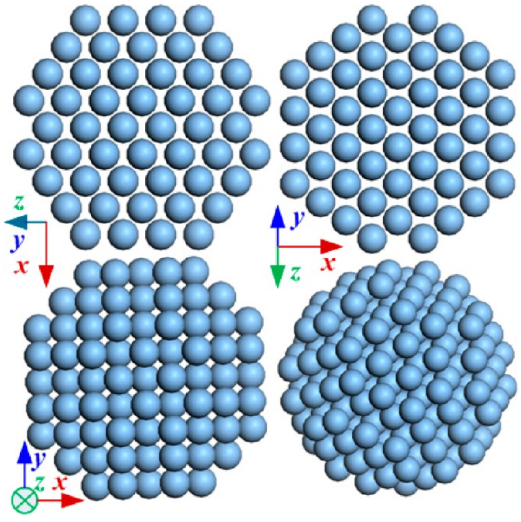

Figure 2. Different atomic configurations of 2 nm Ag particle.

nanoscale welding process. The Ag nanoparticle with 2 nm diameter, including 238 atoms, is face centered cubic (FCC) structure with lattice parameter of 4.0857 Å. And in Figures 1 and 2, as the simulation model, each blue dot represents an Ag atom.

As the MD simulation, the key of calculations is the selection of the interatomic force field. It determines the work load, accuracy of simulation results, and approximate extent between the calculation model and the real system. So MD simulations are performed under the powerful COMPASS (condensed-phase optimized molecular potentials for atomistic simulation studies) force field. It is a parameterized, tested, and validated first ab initio force-field,[26,27] which enables an accurate prediction of condensed matter physics.[28−31] The total potential energy of system includes the valence terms and non-bonded interaction terms, and the valence terms are composed of diagonal term E_{bond} and off-diagonal cross coupling term E_{cross}, which are given by the following functions:

$$E_{total} = E_{valence} + E_{non\text{-}bond} = E_{bond} + E_{cross} + E_{non\text{-}bond} \quad (1)$$

$$\begin{aligned} E_{bond} &= E_b + E_\theta + E_\phi + E_\chi \\ &= \sum_b [K_2(b - b_0)^2 + K_3(b - b_0)^3 + K_4(b - b_0)^4] \\ &+ \sum_\theta [H_2(\theta - \theta_0)^2 + H_3(\theta - \theta_0)^3 + H_4(\theta - \theta_0)^4] \\ &+ \sum_\phi [V_1(1 - \cos\phi) + V_2(1 - \cos 2\phi) \\ &+ V_3(1 - \cos 3\phi)] \\ &+ \sum_\chi K_\chi(\chi - \chi_0)^2 \end{aligned} \quad (2)$$

$$\begin{aligned} E_{cross} &= E_{bb'} + E_{b\theta} + E_{b\phi} + E_{\theta\theta'} + E_{\theta\theta'\phi} \\ &= \sum_{b,b'} F_{b,b'}(b - b_0)(b' - b_0') \\ &+ \sum_{b,\theta} F_{b,\theta}(b - b_0)(\theta - \theta_0) \\ &+ \sum_{b,\phi} (b - b_0)[F_{b,\phi}^{(1)}(1 - \cos\phi) + F_{b,\phi}^{(2)}(1 - 2\cos\phi) \\ &+ F_{b,\phi}^{(3)}(1 - 3\cos\phi)] \\ &+ \sum_{\theta,\theta'} F_{\theta,\theta'}(\theta - \theta_0)(\theta' - \theta_0') \\ &+ \sum_{\theta,\theta'\phi} F_{\theta,\theta'\phi}(\theta - \theta_0)(\theta' - \theta_0')\cos\phi \end{aligned} \quad (3)$$

$$E_{non\text{-}bond} = E_{LJ} + E_{elec} = \sum_{i,j} \varepsilon_{ij}\left[2\left(\frac{r_{ij}^0}{r_{ij}}\right)^9 - 3\left(\frac{r_{ij}^0}{r_{ij}}\right)^6\right] + \sum_{i,j} \frac{q_i q_j}{\varepsilon_0 r_{ij}} \quad (4)$$

Here, E_b, E_θ, E_ϕ, and E_χ represents bond, angle, torsion, and out-of-plane angle coordinates, and $E_{bb'}$, $E_{b\theta}$, $E_{b\phi}$, $E_{\theta\theta'}$, and $E_{\theta\theta'\phi}$ gives cross-coupling term between internal coordinates, respectively. The non-bonded term $E_{non\text{-}bond}$ includes L-J 9-6 potential function for the vdW interaction E_{LJ} and a Coulomb term for electrostatic interactions. It is used for interaction between pairs of atoms that are separated by three or more intervening atoms or those that belong to different molecules.

During MD simulation of nanoscale soldering process, the change in energy is accomplished through the so-called thermal process. So the initial velocities are distributed by Maxwell−Boltzmann. However, Maxwell−Boltzmann distribution is statistics about a large number of atoms with greater fluctuation results. To reduce the energy fluctuation, extending the simulation time is the solution when the number of atoms is small. So time step of 5 fs was set in simulation and Velocity Verlet was chosen as integration method of simulation computation. In the simulations, taking into the size of different materials, the *x*, *y*, and *z* direction of Ag nanoparticle, *y* and *z* direction of SWNTs, and *z* direction of silicon substrate should be imposed by non-periodic boundary. Conversely, the periodic boundary conditions should be imposed on *x* direction of SWNTs, *x* and *y* direction of Si substrate. Considering the stability of SWNTs and bulk silicon

dx.doi.org/10.1021/am405114n | ACS Appl. Mater. Interfaces 2014, 6, 2044−2050

substrate, and the characteristics of periodic boundary, the motion of atoms was constrained in the direction with periodic boundary. At the same time, the simulation box was imposed by non-periodic boundary. For each atomic model, within a cutoff distance of 9.5 Å, the simulation process was performed under the constant *NVT* (*N* is the number of atoms in the system, *V* gives the volume, *T* represents the temperature) ensemble. An Andersen thermostat was chosen in MD simulation. During nanosoldering simulation process, for further analysis of structural properties and atomic configurations, the atomic model was equilibrated to a stable state for 200 ps and the system was left undisturbed in 200 ps constant energy simulation to store the coordinates and velocities of all atoms.

3. RESULTS AND DISCUSSION

Because of the initial velocities of all atoms being randomly distributed in accordance with Maxwell−Boltzmann, we exported the velocity autocorrelation function $C_v(t)$ in eq 5 to verify if the initial velocities have a great impact on the simulation results.

$$C_v(t) = \langle V_i(0) \cdot V_i(t) \rangle \quad (5)$$

Figure 3 shows that the values of $C_v(t)$ tend to zero at the temperature of 900 K, which indicates that the velocities of

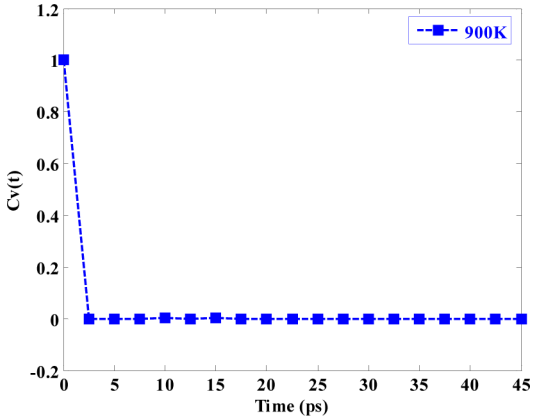

Figure 3. Relationship between $C_v(t)$ and time at the temperature of 900 K.

atoms have no relationship with the initial values. Also, in the subsequent simulation for accumulating data, it indicates that the initial values cannot impact the relevant physical information of these atoms, which can ensure the accuracy, repeatability, and reliability of the data.

The melting of nanosolder plays an important role in the nanosoldering process. Because of the high surface energy of nanoparticle, considering the size effect about the melting temperature, the accurate melting temperature and the intuitional melting process of 2 nm Ag particle can be obtained by MD simulation. Figure 4 gives the corresponding relationship between potential energy and temperature, which shows that the potential energy monotonically and linearly changes with temperature at specific time range. Since the atomic spacing in the liquid state is greater than the distance in solid state, the potential energy significantly changes, resulting mutation in the potential value. Consequently, as the 2 nm Ag particle, the approximate temperature of 605 K could be got from the step point, and the nanoparticle also achieve the transition from the solid phase to liquid phase. This is mainly caused by the high proportion of surface atoms of nanoparticles. Compared with the internal atoms, surface atoms

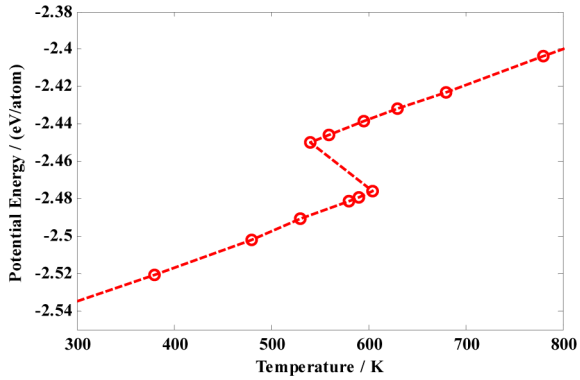

Figure 4. Relationship between potential energy and temperature about 2 nm Ag particle.

have smaller numbers of the nearest neighbor atoms. The surface atoms are weekly bound by the internal atoms, and their thermal motions are less constrained. So nanoparticles have lower melting point than bulk materials with 1234 K melting temperature. Simultaneously, Figure 5 shows the nanoparticle

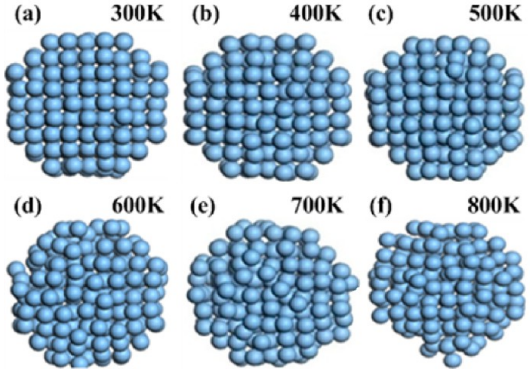

Figure 5. Snapshots for atomic melting configuration of 2 nm Ag particle at different temperature.

atomic configuration of the melting process. When the temperature is relatively low from 300 K to 500 K, all atoms arrange in an orderly and regular shape, which indicates that the nanoparticle is in the solid state. As the temperature increases to 600 K, which is close to the melting point, some atoms become disordered, which indicates the pre-melting process of nanoparticle due to high surface energy. With the temperature continuing to rise, the atomic configurations of nanoparticle are more chaotic without the original regular structures, and the nanoparticle is in the liquid state from Figure 5e to f. So the melting process of nanoparticle is the transition process of atomic structures from order to disorder. Because of the role of surface tension, it is also found that the liquid nanoparticle can automatically reduce to spherical structures, and the Ag atoms only vibrate and rotate near the balance position under the role of metal bonds.

On the basis of the nanosoldering process model of CNTs shown in Figure 1, Figure 6 presents the results of time averaged interconnection configurations of SWNTs at a temperature of 900 K. We obtained interconnections between five pairs of SWNTs with the following chiral indices: (5,5)−(5,5), (8,8)−(8,8), (9,9)−(9,9), (10,10)−(10,10), (15,15)−(15,15), which are all metallic carbon nanotubes and have the same chiralities of armchair type (the specific structural

dx.doi.org/10.1021/am405114n | ACS Appl. Mater. Interfaces 2014, 6, 2044−2050

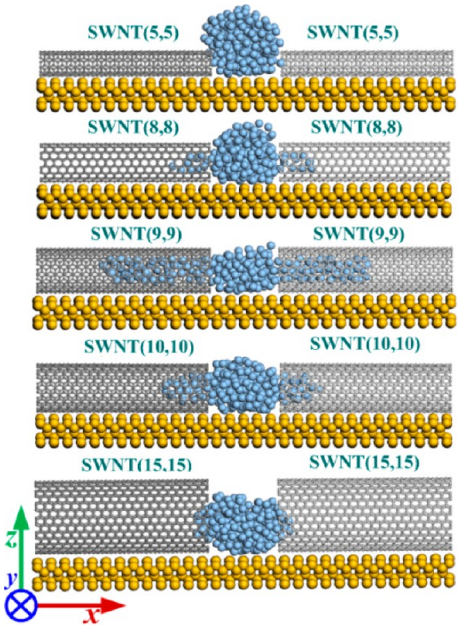

Figure 6. Time-averaged configurations of different pairs of SWNTs at a temperature of 900 K.

information is summarized in Table 1). Obviously, the interconnection configurations highly depend on the diameter of the SWNTs. Ag atoms are dragged into the nanotubes, which is not observed in (5,5)−(5,5) system. As the diameter of SWNT becomes large, some atoms migrate into the nanotube and form the structures of Ag nanowires. However, the length of nanowires encapsulated in the SWNT does not become longer with the increase in diameter. And in our simulation results, the core filling structures in (9,9)−(9,9) system is obvious with the longest length of nanowires. These configurations mainly depend on the thermodynamic properties of nanosolder and the interaction force between Ag atoms and C atoms. At the same temperature, the kinetic energy of the atoms and the potential energy between the Ag atoms are considered to be equal. Consequently, the length of core filling nanowires mainly depends on resultant forces between Ag atoms and the distal suspension C atoms of SWNTs. To illustrate the interaction, Figure 7 shows the positional relationship between Ag atom and the distal suspension C atoms of SWNT. When the diameter of the SWNT is smaller, and the Ag atom is close to the end plane of SWNT, for example, in (5,5)−(5,5) system, the Ag−C distance l_{Ag-C} becomes smaller to a certain extent with the manifestation of the repulsive force between Ag atom and C atoms. So Ag atom can not be captured into the nanotube without the core filling structures. In contrast, when the distance l_{Ag-C} and the angle β become larger with the increase in diameter of SWNT, the interaction between Ag atom and C atom is dominated by composition of attractive forces, with the Ag atoms chain encapsulated into the SWNT. And with the further increase of the diameter of SWNT, because of larger distance l_{Ag-C} and

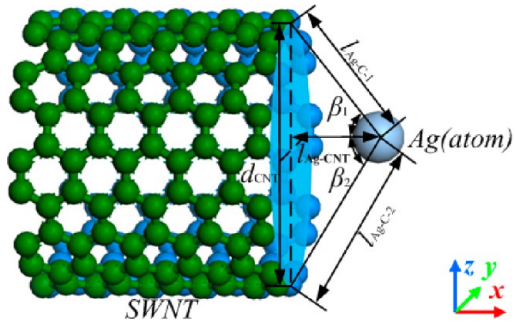

Figure 7. Positional relationship between Ag atom and the distal suspension C atoms of SWNT.

angle β, the attractive forces and their horizontal components will become weaker with the results of the shorter length of Ag nanowires, such as (15,15)−(15,15) system. At the same time, in order to indicate the size of the attractive forces, the nanosoldering processes about (9,9)−(8,8), (9,9)−(9,9), (9,9)−(10,10) systems, are studied in our simulation researches with the dominant results in Figure 8. The length of Ag

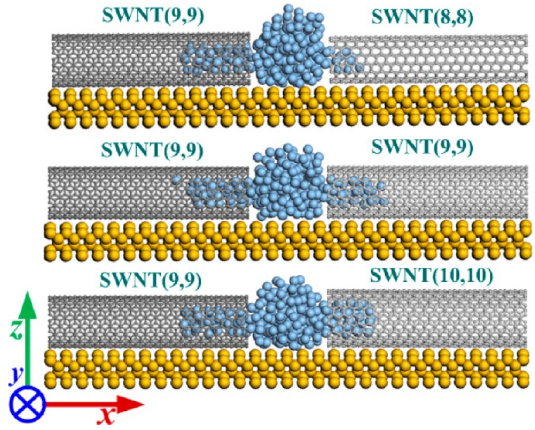

Figure 8. Snapshots for time averaged configurations of different pairs of SWNTs with armchair type at a temperature of 800 K.

nanowires in (9,9)−(9,9) system is longer than the length in other systems. In the (9,9)−(9,9) system, the length of the left core filling structure is nearly equal to the right length. Among the five pairs of SWNTs with the same chiral indices, Figure 8 fully illustrates that the largest trapping forces become the dominant mechanism as the longest length of Ag nanowires in nanotube.

However, in nanosoldering simulations, the shortest length of Ag nanowires appears in the (15,15)−(15,15) system because of minimal capture forces of both sides of SWNTs for Ag atoms. And in the case of the small attractive forces, the distance between C atoms and Ag atoms will affect the changes of forces to influence the interconnection configuration of SWNTs. As this situation, if the position of nanoparticle is changed to near the left nanotube, and the initialization nanosoldering configuration is set, Fig.9 shows the initial and

Table 1. Dimensions of Each SWNT with Different Spiral Vector Parameters

	(5,5)	(8,8)	(10,7)	(9,9)	(10,8)	(11,8)	(10,10)	(15,0)	(15,15)
diameter (Å)	6.78	10.85	11.59	12.20	12.23	12.94	13.56	11.74	20.34
length (Å)	49.19	49.19	49.10	49.19	49.25	49.15	49.19	46.86	49.19

dx.doi.org/10.1021/am405114n | ACS Appl. Mater. Interfaces 2014, 6, 2044−2050

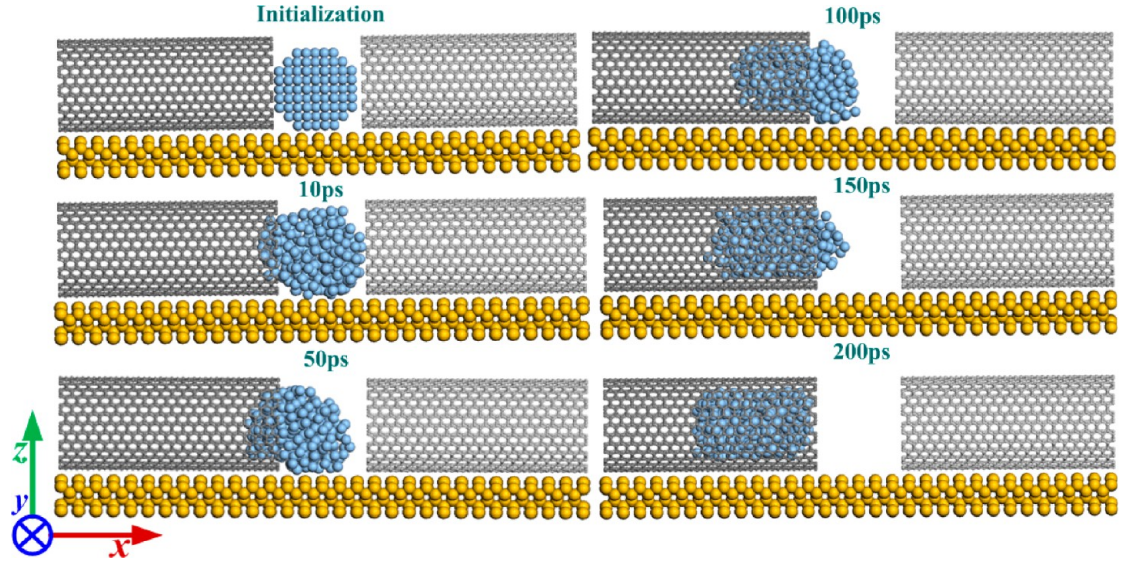

Figure 9. Snapshots for instantaneous configurations of (15,15)−(15,15) system at the temperature of 800 K.

instantaneous configurations of (15,15)−(15,15) SWNTs system at the temperature of 800 K. From the intuitive evolution atomic configurations, the melted nanoparticle exhibits good fluidity, and is sucked into the left nanotube with increasing simulation time. The main reasons of the phenomenon are that Ag atoms have stronger thermal dynamics properties at a higher temperature, and can keep agglomeration owing to stronger metal bonds. The forces of the left and right sides are in unbalanced state. It becomes the one of the pivotal reasons that the whole nanoparticle can move to the left SWNT due to large surface energy for keeping the minimization of system energy.

The connection configurations are analyzed about different pairs of SWNTs with armchair type. However, as the metallic CNT, to investigate the relationship between the connection configuration and spiral vector, the different SWNTs with zigzag and spiral type (the specific structural information is summarized in Table 1) are considered in simulations. For excluding the influence of diameter, Figure 10 presents the results of the time averaged interconnection configurations between different pairs of SWNTs with similar diameter at a temperature of 800 K. There are not significant differences between configurations shown in Figures 8 and 10. At the same time, in the simulation, the evolution of atomic configuration between metallic SWNT (9,9) and semiconducting SWNT (10,8), is also performed under the same simulation diameters, which is shown in Figure 11. Though the atomic structures in left SWNT are loose in the simulation time of 100 ps, the tight atomic structures are accomplished in 200 ps and the final interconnection configuration is similar to that in Figures 8 and 10. Consequently, the interconnection configurations have no relationship with the chirality of SWNTs, and it mainly depends on the diameter of SWNTs.

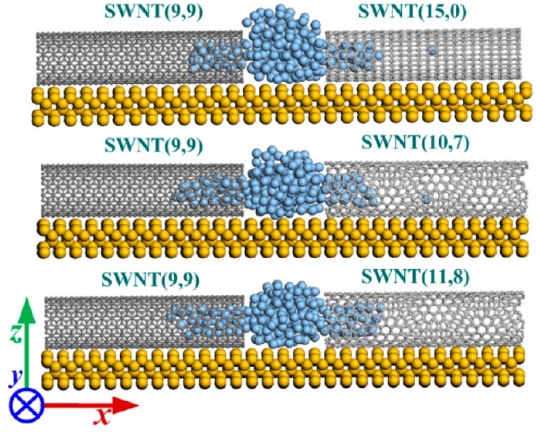

Figure 10. Snapshots for time averaged configurations of different pairs of SWNTs with zigzag and spiral type at a temperature of 800 K.

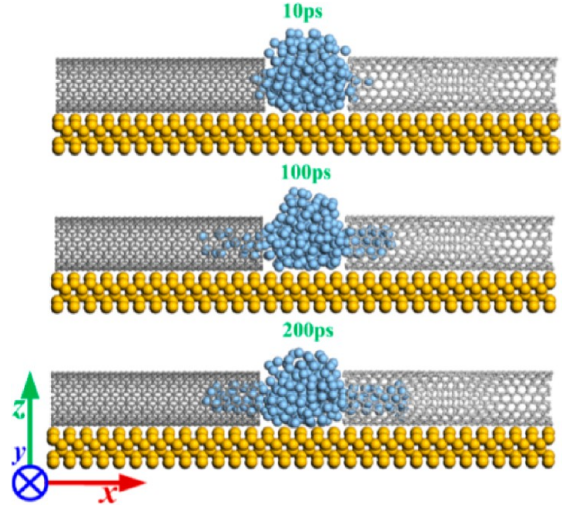

Figure 11. Snapshots for time averaged configurations of (9,9)-(10,8) system at a temperature of 800 K.

Through the above analysis, the interaction between Ag atoms and C atoms seriously affects the connection configuration during nanosoldering. And considering the interconnection configuration of (9,9)-(9,9) SWNTs system at the temperature of 900 and 800 K, shown in Figures 6 and 8, respectively, the interconnection of SWNTs also depends on the nanosoldering temperature. And snapshots for interconnection configuration of SWNTs system from 700 to 1000 K

are shown in Figure 12. At the specific temperature, below the melting point 1234 K of bulk silver material, the nanosolder can

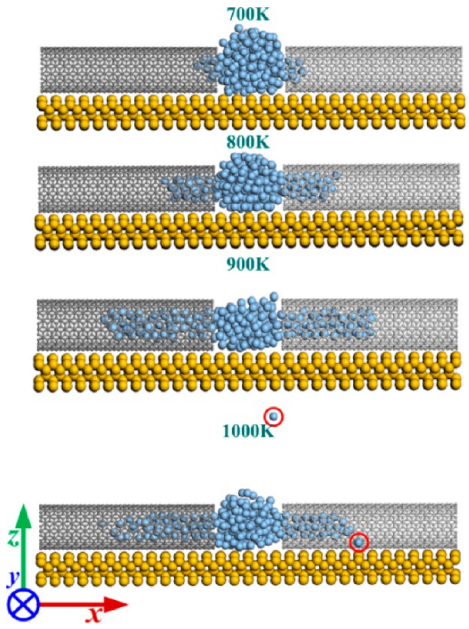

Figure 12. Snapshots for connection configuration of (9,9)−(9,9) system at different temperature.

accomplish transition from solid state to liquid state, and the phenomenon of imbibitions can occur with the core filling nanowires structures. As the temperature increases, more Ag atoms will enter the SWNTs to form a continuous chain, and less Ag atoms can remain in the gap between SWNT and SWNT with the tight atomic structures because of strong metal bonds. In addition, Figure 12 is also noted that the length of nanowires at 1000 K is almost equal to that at 900 K with relatively loose structures. At the temperature of 1000 K, individual Ag atoms, marked in red circles, get rid of the shackles of the other atoms and escape to distant places. The main reason is that the role of the metal bonds is weak. And the thermal motions of the metal atoms are strengthened with small limitations in the case of a higher temperature. So, at the higher temperature, the left length of core filling structures is not equal to the right length because of the stronger thermal dynamics properties and the randomness of the movement of Ag atoms. Consequently, the temperature strongly effects the interconnection of CNTs, and controlling the reasonable nanosoldering temperature would facilitate change the interconnection configuration to improve the mechanical strength.

In the simulation, to directly observe the forming process of interconnection, the atomic evolution connection configurations of (9,9)−(9,9) SWNTs system are exported at different heating time during nanosoldering process, which are shown in Figure 13. Initially, the Ag atoms become disordered in the molten state. Then, these Ag atoms are dragged into nanotube and continuous chain is encapsulated in SWNTs without loose atomic configuration owing to the role of metal bonds. Given enough time, the length of nanowires would increase no longer in the MD simulation process, which also indicates the system is in the stable state. Simultaneously, the interconnection configuration, which can effectively improve the interconnection strength, is in good condition. So, heating time also plays an important role in nanosoldering process.

4. CONCLUSIONS

Because of high surface energy, the melting point of 2 nm silver solder is about 605 K below the melting temperature of Ag bulk material. In the nanosoldering process simulations about SWNTs, Ag atoms may be dragged into the nanotubes to form different connection configuration, which has no apparent relationship with the chirality of SWNTs. Additionally, the length of core filling nanowires does not become longer with the increasing diameter of SWNT, which mainly depends on the metal bonds and the interactions between the Ag atoms and the distal C atoms of SWNTs. At a higher temperature, continuous Ag atoms chain can be easily encapsulated in the SWNT under the larger trapping forces and weaker metal bonds. However, when the nanoparticle is near to the one of SWNTs in unbalanced position, even small, even if the attractive forces are small between C atoms and Ag atoms, the melted nanoparticle with good fluidity can be sucked into the adjacent nanotube. In nanosoldering process, as the heating

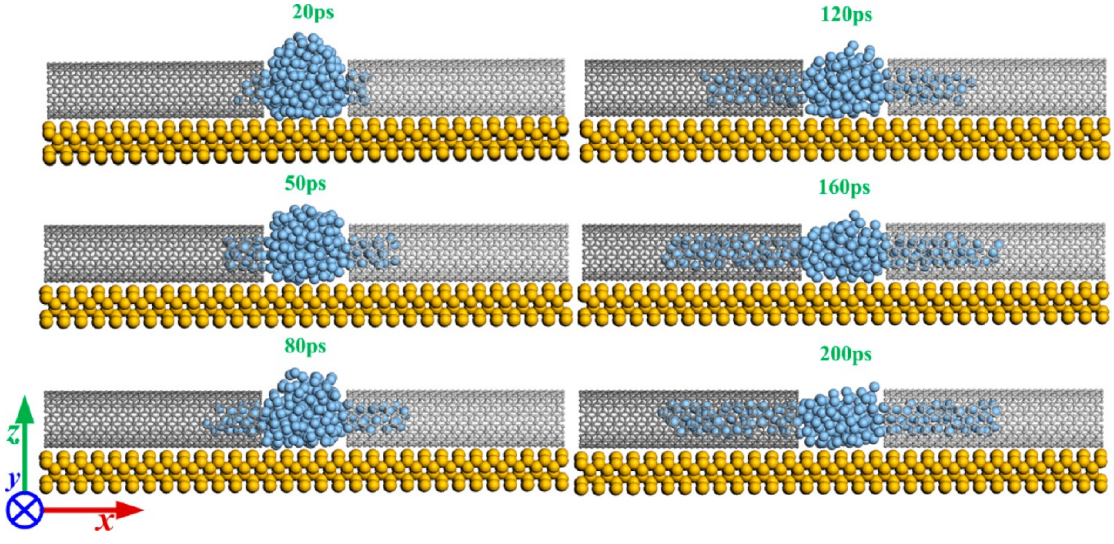

Figure 13. Snapshots for instantaneous configurations of (9,9)−(9,9) system at the temperature of 900 K.

temperature and time respectively increases, more Ag atoms can enter the SWNTs with longer Ag nanowires. Because of strong metal bonds, less Ag atoms can remain with the tight atomic structures in the gap between SWNT and SWNT. Hopefully, understanding the influence of various factors will be propitious to guide high-quality nanosoldering process.

■ ASSOCIATED CONTENT

Supporting Information

Plots with evolution of configurational energy and temperature, the snapshots for nanosolering configuration with longer heating time, energy fluctuation with different time step, and velocity autocorrelation function. This material is available free of charge via the Internet at http://pubs.acs.org/.

■ AUTHOR INFORMATION

Corresponding Authors

*E-mail: yljtj@hit.edu.cn (L.J.Y).
*Tel.: +86 451 86403380. Fax: +86 451 86402755. E-mail: cuijianlei2010@hit.edu.cn (Y.W).

Notes

The authors declare no competing financial interest.

■ ACKNOWLEDGMENTS

This project was supported by the National Natural Science Foundation of China (90923041, 51275122), the Key Laboratory of Micro-systems and Micro-structures Manufacturing (Harbin Institute of Technology), Ministry of Education (HIT.LOF.2011041), the Fundamental Research Funds for the Central Universities (HIT.NSRIF.201171) and the 111 Project of China (B07018). All the authors gratefully acknowledge their support.

■ REFERENCES

(1) Semiconductor Industry Association. International Technology Roadmap for Semiconductors, 2012. http://public.itrs.net/.
(2) Steinhogl, W.; Schindler, G.; Steinlesberger, G.; Engelhardt, M. *Phys. Rev. B* **2002**, *66*, No. 075414.
(3) Li, J.; Ye, Q.; Cassell, A.; Ng, H. T.; Stevens, R.; Han, J.; Meyyappan, M. *Appl. Phys. Lett.* **2003**, *82*, 2491−2493.
(4) Iijima, S. *Nature* **1991**, *354*, 56−58.
(5) Malapanis, A.; Perebeinos, V.; Sinha, D. P.; Comfort, E.; Lee, J. U. *Nano Lett.* **2013**, *13*, 3531−3538.
(6) Park, W. J.; Choi, K. J.; Kim, M. H.; Koo, B. H.; Lee, J. L.; Baik, J. M. *ACS Appl. Mater. Interfaces* **2013**, *5*, 6802−6807.
(7) Fuhrer, M. S.; Nygård, J.; Shih, L.; Forero, M.; Yoon, Y. G.; Mazzoni, M. S. C.; Choi, H. J.; Ihm, J.; Louie, S. G.; Zettl, A.; McEuen, P. L. *Science* **2000**, *288*, 494−497.
(8) Close, G. F.; Yasuda, S.; Paul, B.; Fujita, S.; Wong, H.-S. P. *Nano Lett.* **2008**, *8*, 706−709.
(9) Sciascia, C.; Castagna, R.; Dekermenjian, M.; Martel, R.; Kandada, A. R. S.; Di Fonzo, F.; Bianco, A.; Bertarelli, C.; Meneghetti, M.; Lanzani, G. *J. Phys. Chem. C* **2012**, *116*, 19483−19489.
(10) Ahmad, M.; Anguita, J. V.; Stolojan, V.; Carey, J. D.; Silva, S. R. P. *ACS Appl. Mater. Interfaces* **2013**, *5*, 3861−3866.
(11) Postma, H. W. C.; Teepen, T.; Yao, Z.; Grifoni, M.; Dekker, C. *Science* **2001**, *293*, 76−79.
(12) Yao, Z.; Postma, H. W. C.; Balents, L.; Dekker, C. *Nature* **1999**, *402*, 273−276.
(13) Mashock, M.; Yu, K.; Cui, S.; Mao, S.; Lu, G.; Chen, J. *ACS Appl. Mater. Interfaces* **2012**, *4*, 4192−4199.
(14) Barman, S. N.; LeMieux, M. C.; Baek, J.; Rivera, R.; Bao, Z. *ACS Appl. Mater. Interfaces* **2010**, *2*, 2672−2678.
(15) Mitsuishi, K.; Shimojo, M.; Han, M.; Furuya, K. *Appl. Phys. Lett* **2003**, *83*, 2064−2066.
(16) Banhart, F. *Rep. Prog. Phys.* **1999**, *62*, 1181−1221.
(17) Krasheninnikov, A. V.; Nordlund, K.; Keinonen, J.; Banhart, F. *Phys. Rev. B* **2002**, *66*, 245403.
(18) Krasheninnikov, A. V.; Nordlund, K.; Keinonen, J. *Phys. Rev. B* **2002**, *65*, 165423.
(19) Heermann, D. W. *Computer-Simulation Methods*; Springer: Berlin, 1990.
(20) Andrew, R. L. *Molecular Modeling: Principle and Practice*; Springer: Berlin, 1996.
(21) Jawalkar, S. S.; Adoor, S. G.; Sairam, M.; Nadagouda, M. N.; Aminabhavi, T. M. *J. Phys. Chem. B* **2005**, *109*, 15611−15620.
(22) Prathab, B.; Aminabhavi, T. M.; Parthasarathi, R.; Manikandan, P.; Subramanian, V. *Polymer* **2006**, *47*, 6914−6924.
(23) Prathab, B.; Subramanian, V.; Aminabhavi, T. M. *Polymer* **2006**, *48*, 409−416.
(24) Terrones, M.; Banhart, F.; Grobert, N.; Charlier, J. C.; Terrones, H.; Ajayan, P. M. *Phys. Rev. Lett.* **2002**, *89*, No. 075505.
(25) Jang, I.; Sinnott, S. B.; Danailov, D.; Keblinski, P. *Nano Lett.* **2004**, *4*, 109−114.
(26) Maple, J. R.; Hwang, M. J.; Stockfisch, T. P.; Dinur, U.; Waldman, M.; Ewig, C. S.; Hagler, A. T. *J. Comput. Chem.* **1994**, *15*, 162−182.
(27) Sun, H. *J. Comput. Chem.* **1994**, *15*, 752−768.
(28) Sun, H. *J. Phys. Chem. B* **1998**, *102*, 7338−7364.
(29) Sun, H.; Ren, P.; Fried, J. R. *Comput. Theor. Polym. Sci.* **1998**, *8*, 229−246.
(30) Rigby, D.; Sun, H.; Eichinger, B. E. *Polym. Int.* **1998**, *44*, 311−330.
(31) Xie, J.; Xue, Q.; Yan, K.; Chen, H.; Xia, D.; Dong, M. *J. Phys. Chem. C* **2009**, *113*, 14747−14752.